JOURNAL OF GEOPHYSICAL RESEARCH, VOL. 112, A07301, doi:10.1029/2007JA012347, 2007

Storm time, short-lived bursts of relativistic electron precipitation detected by subionospheric radio wave propagation

Craig J. Rodger,[1] Mark A. Clilverd,[2] David Nunn,[3] Pekka T. Verronen,[4] Jacob Bortnik,[5] and Esa Turunen[6]

Received 14 February 2007; revised 26 March 2007; accepted 6 April 2007; published 7 July 2007.

[1] In this study we report on ground-based observations of short bursts of relativistic electron precipitation (REP), detected by a subionospheric propagation sensor in Sodankylä, Finland during 2005. In two ~4 hour case study periods from $L = 5.2$, around local midnight, several hundred short-lived radio wave perturbations were observed, covering a wide range of arrival azimuths. The vast majority (~99%) of these perturbations were not simultaneous with perturbations on other paths, consistent with a precipitation "rainstorm" producing ionospheric changes of small spatial sizes around the Sodankylä receiver. The recovery time of these radio wave perturbations are ~1.2 s, which is consistent with the modeled effects of a burst of >2 MeV precipitating electrons. This agrees with satellite observations of the microburst energy spectrum. The energetic nature of the precipitation which produces the FAST perturbations suggests that they should be observable in both day and night conditions. While it is widely assumed that satellite-detected REP microbursts are due to wave-particle interactions with very low-frequency chorus waves, the energy spectra predicted by our current models of chorus propagation and wave-particle interaction are not consistent with the experimentally observed radio wave perturbations presented here or previously reported satellite observations of REP microbursts. The results inferred from both the satellite and subionospheric observations, namely the absence of a large, dominant component of <100 keV precipitating electrons, fundamentally disagrees with a mechanism of chorus-driven precipitation. Nonetheless, further work on the modeling of chorus-driven precipitation is required.

Citation: Rodger, C. J., M. A. Clilverd, D. Nunn, P. T. Verronen, J. Bortnik, and E. Turunen (2007), Storm time, short-lived bursts of relativistic electron precipitation detected by subionospheric radio wave propagation, *J. Geophys. Res.*, *112*, A07301, doi:10.1029/2007JA012347.

1. Introduction

[2] In the more than 4 decades since the discovery of the Earth's Van Allen radiation belts, it has proved difficult to confirm the principal source and loss mechanisms that control radiation belt particles. At geostationary orbits, geomagnetic storms have been found to cause significant variations in trapped radiation belt relativistic electron fluxes, through a complex interplay between competing acceleration and loss mechanisms. *Reeves et al.* [2003] found that geomagnetic storms produce all possible responses in the outer belt flux levels, i.e., flux increases (53%), flux decreases (19%), and no change (28%). Understanding the loss of relativistic electrons is a key part to understanding the dynamics of the energetic radiation belts.

[3] A significant loss mechanism that removes trapped relativistic electrons from the radiation belts is relativistic electron precipitation (REP) into the atmosphere. One common form of REP is relativistic microbursts which are bursty, short duration (<1 s) precipitation events containing electrons of energy >1 MeV [*Imhof et al.*, 1992; *Blake et al.*, 1996]. Observations from the SAMPEX satellite show that REP microbursts occur at about $L = 4–6$ and are observed predominantly in the morning sector. Primarily because of this local time dependence, microbursts have been associated with very low frequency (VLF) chorus waves [*Nakamura et al.*, 2000; *Lorentzen et al.*, 2001b]. Estimates of flux losses due to relativistic microbursts show that they could empty the radiation belt in about a day [*Lorentzen et al.*, 2001a; *O'Brien et al.*, 2004; *Thorne et al.*, 2005]. SAMPEX observations have also shown that REP microbursts are often accompanied by nonrelativistic (>150 keV) microbursts, but the bursts in the two energy channels

[1]Department of Physics, University of Otago, Dunedin, New Zealand.
[2]Physical Sciences Division, British Antarctic Survey, Cambridge, UK.
[3]School of Electronics and Computer Science, Southampton University, Southampton, UK.
[4]Earth Observation, Finnish Meteorological Institute, Helsinki, Finland.
[5]Department of Atmospheric and Oceanic Sciences, University of California, Los Angles, California, USA.
[6]Sodankylä Geophysical Observatory, University of Oulu, Sodankylä, Finland.

0148-0227/07/2007JA012347$09.00

do not exhibit a one-to-one correspondence. Nonrelativistic (>150 keV) microbursts are also of short duration (~0.2–0.3 s) and occur on the dayside [*Anderson and Milton*, 1964; *Datta et al.*, 1996]. Rocket and balloon measurements indicate that the precipitating electrons are primarily in the tens to hundreds of keV range [*Imhof et al.*, 1989; *Reinard et al.*, 1997], with the majority of the precipitated electrons confined to ≈20–120 keV [*Datta et al.*, 1996]. While the original balloon measurements did not include detectors for relativistic electrons, modern balloon campaigns (e.g., MINIS) do make measurements in this energy range, and while reporting long-period relativistic electron precipitation [*Millan et al.*, 2002] they have yet to observe REP microbursts. Owing to the integral flux detectors present on board SAMPEX, limited information on the energy spectra of REP microbursts has been available to date as very few other spacecraft have reported on REP microburst observations. A small number of non-REP microburst energy spectra in the energy range 170–360 keV have been reported from the Science Technologies Satellite (STSAT-I). The spectra can be described using exponential fits [*Lee et al.*, 2005].

[4] SAMPEX-observed REP microbursts are correlated with satellite observed VLF chorus wave activity [*Lorentzen et al.*, 2001b]. The short duration of microbursts, similar to the individual elements in VLF chorus, as well as the similarity in local time (LT) distributions have lead to the widely held assumption that REP microbursts are produced by wave-particle interactions with chorus waves. However, this has yet to be confirmed, and a one-to-one correlation of REP microbursts and chorus elements has yet to be demonstrated. In contrast, one-to-one correlations have been established between nonrelativistic microburst and individual risers in VLF chorus [*Rosenberg et al.*, 1990], providing further impetus to confirm or deny the link between REP microbursts and chorus.

[5] To investigate the energy spectra and hence the source mechanism of REP, we analyze ground-based ionospheric data during periods of high geomagnetic activity when short-lived bursts of precipitation into the upper atmosphere are known to have occurred [*Clilverd et al.*, 2006]. Precipitating electrons with energies >1 MeV will cause increased ionization in the lower ionosphere, with the bulk of the energy deposited below about 65 km. One of the few experimental techniques which can probe ionization changes at these altitudes uses VLF electromagnetic radiation, trapped between the lower ionosphere and the Earth [*Barr et al.*, 2000]. The nature of the received radio waves is largely determined by propagation between these boundaries [e.g., *Cummer*, 2000], termed "subionospheric propagation." Subionospheric VLF propagation allows remote sensing of the upper atmosphere over large regions; these signals can be received thousands of kilometers from the source, where ionospheric modifications lead to changes in the received amplitude and phase. Manmade VLF transmitters provide a well-defined modeling situation due to the known transmitter-receiver locations and fixed frequency operation and near continuous operation [*Barr et al.*, 2000]. Recently, subionospheric propagation probing observed both REP microbursts and slower REP processes, with timescales of tens of minutes, during the January 2005 "MINIS" balloon campaign [*Clilverd et al.*, 2006]. To the best of the authors knowledge, this was the first ground-based observation of microburst REP, to date unreported even by multiple balloon campaigns (e.g., MINIS) that were focused upon this goal.

[6] In this study we examine short-lived VLF perturbations which might be linked to REP microbursts. We compare the ionization decay times produced by modeled chorus-induced precipitation and monoenergetic particle beams with the observed VLF perturbation signatures. Here we concentrate on a limited time period to provide the first detailed analysis of these subionospheric perturbations and the possible linkage to SAMPEX microbursts and to VLF chorus activity.

2. Experimental Setup

[7] In our study we make use of narrow band subionospheric VLF/LF data spanning 20–40 kHz received using an OmniPAL instrument at Sodankylä, Finland (67°N, 26°E, L = 5.3). This receiver site is part of the Antarctic-Arctic Radiation-belt Dynamic Deposition VLF Atmospheric Research Konsortia (AARDDVARK). More information on AARDDVARK can be found at the Konsortia Web site: http://www.physics.otago.ac.nz/space/AARDDVARK_homepage.htm. Figure 1 shows the location of the receiver site (shown by a diamond) and the transmitter-receiver paths that were observed during the event period (transmitter locations are given by the circles). The transmitters examined in this study were the high-powered U. S. Navy transmitters located at Cutler, Maine (with call sign NAA at a frequency of 24.0 kHz), Dakota (NDK, 25.2 kHz), and Iceland (NRK, 37.5 kHz). Here we concentrate on REP microburst observations during two large geomagnetic storms, the first on 21 January 2005, building on the early observations during this event [*Clilverd et al.*, 2006], and the second on 4–5 April 2005. The location of the terminator is also shown as a dotted line for both days, with America daylit during the events. On 21 January 2005 a coronal mass ejection triggered a Kp = 8, Dst = −100 nT geomagnetic storm, leading to the relativistic electron dropout at geosynchronous orbit starting at ~1710 UT. GOES 10 and GOES 12 >2 MeV electron fluxes had decreased by three orders of magnitude by 1800 UT. The coronal mass ejection was associated with a 20 January X7 solar flare and with a solar proton event (SPE) with an unusually hard spectrum [*Seppälä et al.*, 2006], the flux of which had significantly decayed in intensity by the time of the REP activity. In contrast, the geomagnetic storm on 4–5 April 2005 which peaked at local midnight with Kp = 7, Dst = −85 nT, also triggered decreases in the geostationary trapped fluxes starting late on 4 April 2005 but was not associated with any solar proton activity.

3. REP Microbursts in VLF Data

[8] During both of these study periods, the received amplitude of the transmitter signals include many large short-lived spike events of 1–5 dB, both increases and decreases as seen in Figure 2. Figure 2 shows the residual amplitudes that remain after removing the smoothed background with a 5 s filter, which draws out the rapid changes. Similar short-lived large negative and positive perturbations

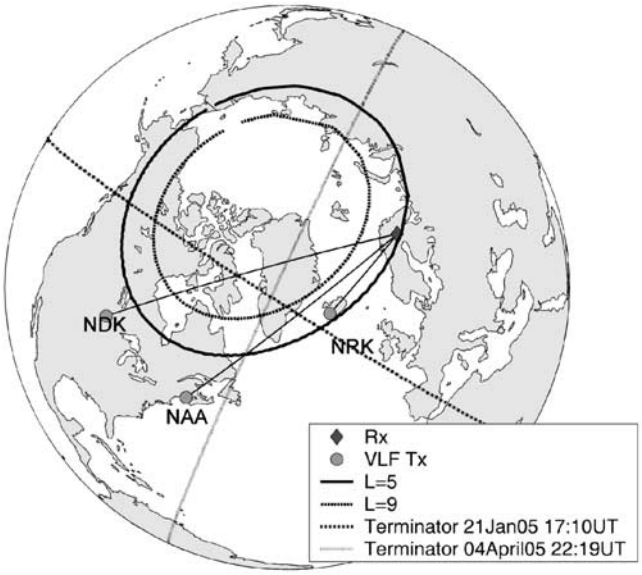

Figure 1. The location of subionospheric propagation paths to the Antarctic-Arctic Radiation-belt Dynamic Deposition VLF Atmospheric Research Konsortia (AARDDVARK) receiver in Sodankylä, Finland.

are also observed in the transmitter phase, representing a phase advance or retardation [e.g., *Watt*, 1967]. These "FAST" short-lived spike events occur during periods of longer timescale "SLOW" REP, which was described by *Clilverd et al.* [2006]. As outlined in that study, none of the other operational AARDDVARK receivers observed FAST perturbations. Over the 4 hour period 1700–2100 UT, 221 FAST perturbations were observed on transmissions from the transmitter NAA and 109 on NDK, i.e., a rough rate of 1 per minute on each of the great circle paths from transmitter to receiver. However, we caution that transforming the observation rate to a precipitation rate is nontrivial, given the current unknowns. The majority of the FAST perturbations are not simultaneous with perturbations on other paths even though they occur during the same periods. An example of this is shown in Figure 3, where FAST perturbations in amplitude are clearly observed on transmissions from both NDK and NAA but with totally independent timing. However, a very small fraction, on the order of ~1–2%, appears to be simultaneous on multiple paths. This behavior is consistent with ionospheric changes with relatively small spatial size, occurring near to the Sodankylä receiver. A useful analogy is a rainstorm, with many small raindrops produced by the same physical process spanning a much larger spatial region. In general, one expects a precipitation-produced ionospheric change located on the transmitter-receiver great circle path and well below the altitude at which VLF reflects to produce a predominantly negative amplitude, negative phase perturbations. However, if the ionospheric conductivity change is located very close to the receiver (<~400 km), particularly if the ionospheric change is particularly large (e.g., as with "VLF sprites" [*Dowden et al.*, 2001]), all combinations of amplitude and phase changes are possible. As there are both large positive and negative perturbations observed in both the amplitude and phase, with low coincidence between the paths, this is highly suggestive of small precipitation-produced ionospheric changes located local to the receiver. Similar spatial sensitivity has been suggested before in the detection of bursts of whistler-induced electron precipitation (Trimpi) only when the bursts occur close to either the transmitter or the receiver and not in the middle of the GCP [*Nunn and Strangeways*, 2000]. It is extremely unlikely that the precipitation is occurring near all three transmitters, as no FAST perturbations are observed at other AARDDVARK sites, in particular that at Ny Ålesund, Svalbard (79°N, 11°E, L = 18.3) [*Clilverd et al.*, 2006]. In addition, the transmitters NDK and NAA are located near $L \approx 3$, significantly outside the satellite observed range of relativistic microburst precipitation. Together these confirm our conclusion that the FAST perturbations are due to precipitation occurring near the Sodankylä receiver.

[9] Figure 3 shows an example of 60 s worth of Sodankylä-received subionospheric amplitude from VLF transmitters on 21 January 2005, plotted at the maximum 0.1 s time resolution. Several well-defined FAST features are evident, each lasting roughly ~1 s, as well as a feature on NDK lasting ~6 s which appears to be made up of multiple discrete pulses. The well-defined FAST features are typical for the short-lived pulses seen during this geomagnetic

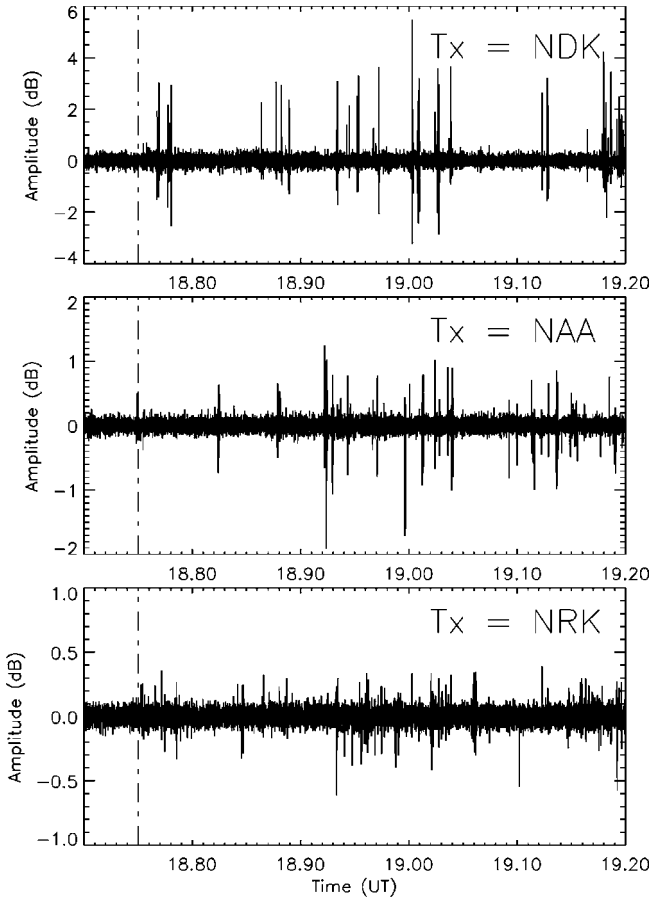

Figure 2. Short-lived amplitude perturbations on subionospheric VLF transmissions received at Sodankylä, Finland, on 21 January 2005.

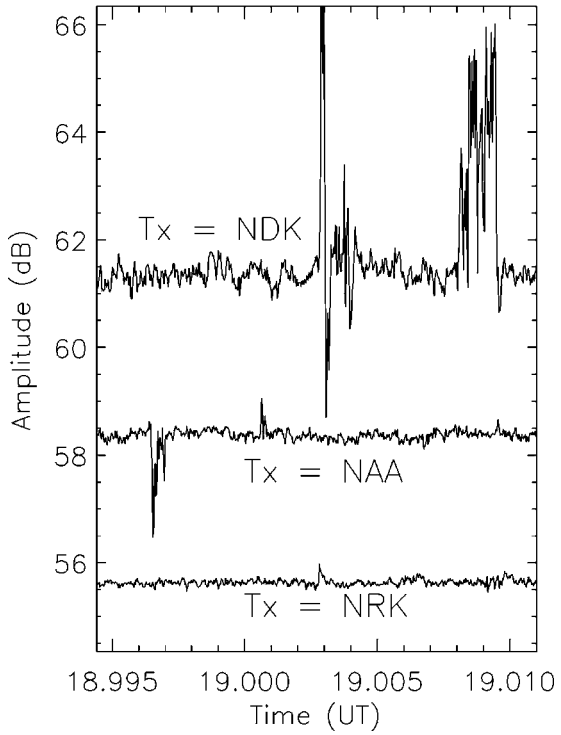

Figure 3. The amplitude of the VLF transmitters received at Sodankylä, Finland, showing a FAST VLF perturbations caused by short-lived bursts of relativistic electron precipitation (REP) on 21 January 2005.

storm, made up of a 0.2 s rise followed by a 0.5 s decay to background amplitude levels. The rapid decay time is highly suggestive of a short-lived highly energetic precipitation burst producing significant additional ionization at ~60 km altitude, the peak altitude for ionization produced by a ~1.5 MeV electron entering the atmosphere [e.g., *Rishbeth and Garriott*, 1969]. It appears that the FAST subionospheric VLF perturbations may be caused by ionization changes produced in the ionosphere through the impact of short-lived bursts of relativistic electron precipitation, which we investigate in more detail in subsequent sections of this study. Note, however, that we cannot conclude that these short-lived bursts of relativistic electron precipitation are SAMPEX-like REP microbursts, which will require further investigation and preferably confirmation by combined satellite/ground-based data.

[10] Further evidence for the energetic nature of the subionospherically observed REP events which occurred on transmissions from NDK on 4 April 2005 are shown in Figure 4 which contrasts the typical decay times for this day and the events from 21 April 2005. The 21 January 2005 perturbation shown in Figure 4 occurred at 1716:43 UT and the 4 April 2005 perturbation occurred at 2218:49 UT. While the FAST perturbations seen on 4 April 2005 are fundamentally similar to the perturbations observed on 21 January 2005, the decay times of the 4 April 2005 events are a factor of ~1.5 longer. On the 21 January 2005 the typical decay time is 0.8 s with a standard deviation of 0.25 s. In contrast, on the 4 April 2005 the typical decay time is 1.2 s with a standard deviation of 0.35 s. The shorter decay times observed on 21 January 2005 is consistent with some masking of higher altitude ionization changes from subionospheric detection on 21 January 2005 due to the proton precipitation continuing on from the 20 January 2005 SPE. This provides strong evidence that both sets of FAST perturbations are produced by short-lived bursts of REP, with the "real" perturbation decay time being ~1.2 s when not masked by ionization produced from proton precipitation.

[11] The OmniPAL instrument includes a sferic suppression algorithm to improve the signal to noise levels in the data. However, this slows the response of the instrument to sudden changes, such that an impulsive step in the true transmitter amplitude results in a gradual rise over 0.2–0.3 s [*Dowden et al.*, 2001]. Thus the observed 0.2 s rise time for the FAST VLF perturbations indicate only that the precipitation lasted ≤0.2 s, after which the additional ionization produced in the lower ionosphere relaxes over ~1.2 s.

[12] In considering the origin of the VLF burst events, we should investigate mechanisms other than very energetic electron precipitation as potential causes. Sudden impulsive events such as lightning-radiated sferics could produce a noise spike that appear as short-lived bursts of VLF noise, especially if the lightning occurred close enough to the receiver location to dominate the transmitter signal power. In general, such events are very uncommon with OmniPAL-style coherent receivers, which are locked to the transmitter so as to better reject lightning noise. The timescales of such breakthroughs are of the order of 0.5 s, which is similar to the events reported here. However, sferic breakthrough would cause a change in signal amplitude on all of the channels at the same time and would also only lead to increases in measured amplitude. Neither of these characteristics is observed in the short-lived VLF perturbation events described in this paper. No other candidate mechanism for short-lived VLF perturbation events appears significant, other than lightning breakthrough and low-altitude ionospheric modification.

4. Monoenergetic Beam VLF Perturbations

[13] As an initial step in modeling the subionospheric bursts, we assume that the FAST VLF perturbations are due to short-lived precipitation bursts of monoenergetic electrons at high energies and do not assume that any specific wave mechanism causes the precipitation. Because there is a >1 order of magnitude difference between the ionization decay times at 60 km and at 70 km altitude [*Rodger and McCormick*, 2006] the decay time of the observed perturbations allows us to use the atmosphere as an energy spectrometer, providing some discrimination as to the nature of the precipitating particles. We start by considering the decaying time signature of a VLF perturbation produced by a 0.1 s burst of monoenergetic REP with a flux of 100 el cm^{-2} s^{-1} sr^{-1}, similar to the fluxes of REP microburst fluxes reported by SAMPEX. In order to describe the atmospheric impact of the energetic electron precipitation, we make use of the Sodankylä Ion Chemistry model. The Sodankylä Ion Chemistry (SIC) model is a one-dimensional (1-D) chemical model designed for ionospheric *D* region studies, solving the concentrations of 64 ions, including 28 negative ions, and 13 neutral species

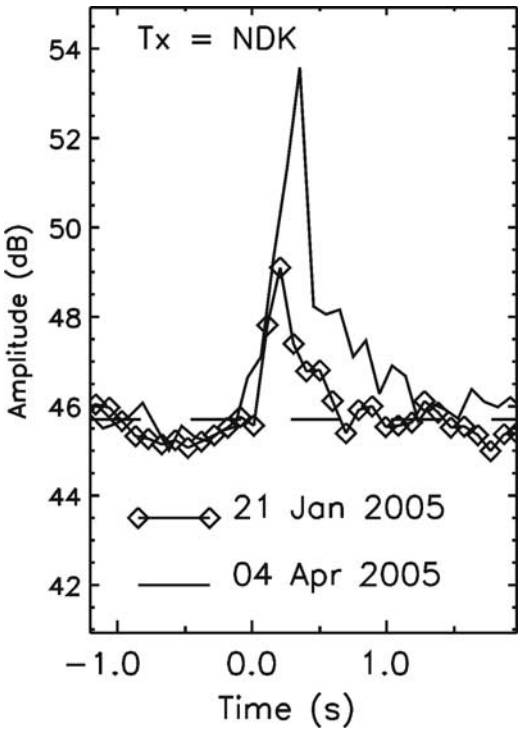

Figure 4. Examples of FAST VLF perturbations on NDK received at Sodankylä caused by REP on 21 January 2005 (line marked by diamonds) and 4 April 2005 (dashed line), showing the contrast between the typical decay times.

at altitudes across 20–150 km. In the SIC model over 300 reactions are implemented, plus additional external forcing due to solar radiation (1–422.5 nm), electron and proton precipitation, and galactic cosmic radiation. Initial descriptions of the model are provided by *Turunen et al.* [1996], with neutral species modifications described by *Verronen et al.* [2002]. A detailed overview of the current model was given by *Verronen et al.* [2005]. For our current study, the primary modeling parameters as those which relate the relaxation time of the ionosphere after the precipitation, i.e., the electron-ion recombination rates and electron-to-neutral attachment rates. These are listed in the work of *Turunen et al.* [1996]. The SIC model runs were undertaken for polar night conditions appropriate for 1700 UT on 21 January 2005 at a location of (69°N, 22.5°E), i.e., close to our receiver in Finland.

[14] Figure 5 shows the time varying electron number density profiles determined from the SIC model produced by a 2 MeV monoenergetic electron beam. The largest changes in electron density occur over the altitudes from ~50 to 63 km, causing increases of >20 times ambient levels. Below ~55 km the increases last less than 0.5 s, due to the high number densities at lower altitudes. The lifetime of the ionization change is determined by a combination of the energy spectra, which drives the altitude-dependent ionization rates, and the chemical recovery times, which become progressively longer with increasing altitudes. This then drives the response of the subionospheric VLF signatures, as has been earlier considered for lightning-induced whistler driven precipitation [*Rodger et al.*, 2004].

[15] The time-varying electron number density altitude profiles were applied to the subionospheric VLF wave propagation code MODEFNDR combined with linear scattering theory [e.g., *Nunn and Strangeways*, 2000; *Rodger et al.*, 2004]. VLF propagation from the source transmitter to a 3-D spatial grid used to model the modified region is computed using modal theory and the Naval Ocean Systems Center (NOSC; San Diego, USA) MODEFNDR code [*Morfitt and Shellman*, 1976]. The MODEFNDR code returns all the parameters of the subionospheric VLF modes as described by *Wait* [1996]. MODEFNDR receives as inputs the frequency, as well as ionospheric and geomagnetic parameters. As an example, for the NDK-Sodankylä path the primary parameters are frequency of 25.2 kHz, great circle path length 6.57515 Mm, and an ionosphere electron density described by a Wait ionosphere [*Wait and Spies*, 1964] with $H' = 83.7$ km and $\beta = 0.41$ km^{-1}. Here H' is a reference height, and β reflects the sharpness of the electron density profile. Then, assuming horizontal homogeneity, but taking into account the curvature of the Earth, the program calculates the appropriate full wave reflection coefficients for the waveguide boundaries and searches for those complex modal angles which give a phase change of 2π across the guide. At each grid point, linear scattering theory furnishes an effective current $\underline{J}_{eff}(\underline{r})$ which acts as the source of the scattered field $\underline{E}_s$. The linear Born theory of 3-D VLF scattering from an ionospheric plasma perturbation is fully described by *Nunn* [1997]. The current version of the code neglects all components of the conductivity tensor except the *zz* component, amply justified to an overall accuracy of order a few percent [*Clilverd et al.*, 1999]. The vertical electric field at the receiver is computed for each elementary volume of the modified region using MODEFNDR, summed over the total modification volume to give the total scattered field, and thus the observed VLF perturbation at a given time.

[16] This process is then repeated for each of the time-varying electron number density altitude profiles, producing the resulting time-varying amplitude changes calculated for propagation modification located on the NDK-Sodankylä path. We represent the modified ionosphere by a 50 km diameter patch located 200 km away from Sodankylä on the transmitter-receiver path. Both the location and size of the precipitation are somewhat arbitrary, chosen to reflect the "small" and "close" requirements for our "raindrop" observations. For our current study the specific location and spatial size are not important to the conclusions of the study, as we focus only upon the time decay signature of the VLF perturbation, determined by the decay of the precipitation-produced ionization density increases. Owing to the very large ionization increases produced by the very energetic precipitation the absolute amplitude changes determined by MODEFNDR are unreliable because nonlinear scattering becomes highly significant. However, the calculated time profile will be a valid determination of the signature of the chorus VLF perturbation. Owing to the uncertainties in range and patch size, we only consider the time decay and normalize all perturbations to the peak value.

[17] As noted above, more energetic electrons penetrate deeper into the atmosphere, where the electron density increases produced by the precipitation will decay away more quickly than electron density increases occurring at higher altitudes, leading to differences in the decay times of the VLF perturbations. For example, there is a factor of

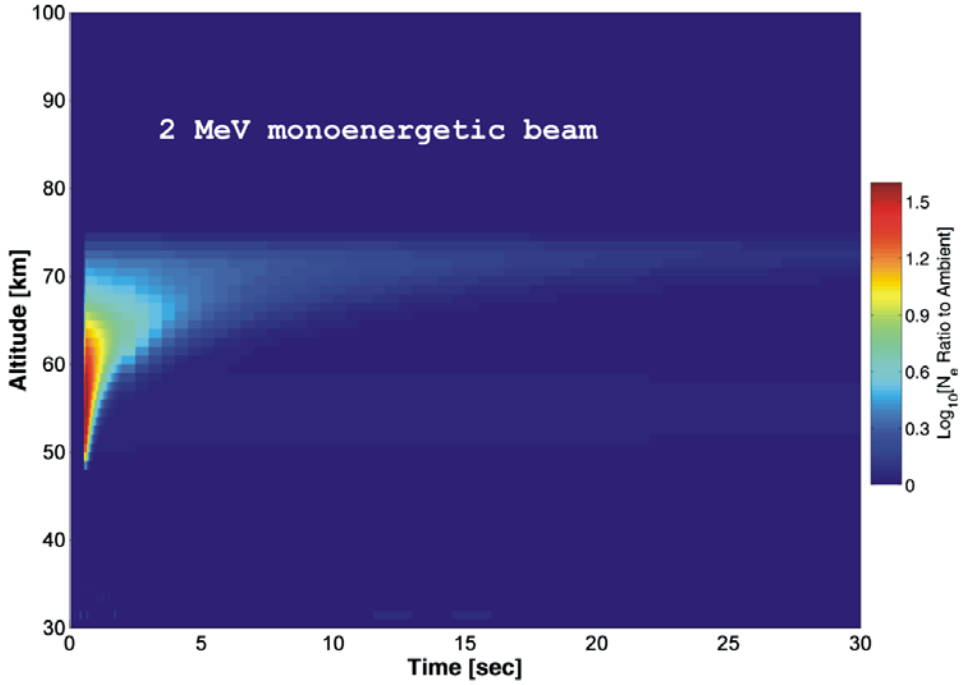

Figure 5. Time varying electron number density calculated by the SIC model, showing the decay of the ionospheric change produced by a 2 MeV monoenergetic beam.

~15 difference between the decay times of ionization at 60 km and at 70 km altitude [*Rodger and McCormick*, 2006], with higher ionization decaying more slowly. The decay time observation technique we employ here treats the atmosphere as an energy spectrometer, providing important energy discrimination. While there are uncertainties in *D* region chemical modeling, the penetration altitude and decay time technique has previously been successfully applied to red sprites [*Nunn and Rodger*, 1999] and low-medium energy electron precipitation [*Rodger et al.*, 2004]. In addition, the accuracy of the SIC model to energetic precipitation has been successfully tested through the modeling of solar proton events [e.g., *Verronen et al.*, 2005] which penetrate deeply into the atmosphere much as relativistic electrons do. We therefore examine the decay times of VLF perturbations produced by mononenergetic beams of various energies. Figure 6 shows calculated decay times of VLF perturbations produced by 1, 2, and 3 MeV beams. These decay times should be contrasted with that for a representative experimentally observed FAST perturbation (light line) which occurred on transmissions from NDK at 2136:54.80 UT on 5 April 2005. Even in the case of simple monoenergetic beams, it is clear that very high energies are necessary in order to reproduce the experimental decay times. The 1 MeV beam leads to a significant negative "undershoot," largely caused by ionization located >70 km, while the 2 and 3 MeV monoenergetic precipitating beams are reasonably close to the observed data.

[18] On the basis of this comparison, we conclude that the experimentally observed VLF perturbations are probably driven by precipitation containing a significant population of highly relativistic populations, principally from energies greater than about 2 MeV, and very little from lower energies. We note that this is roughly consistent with the SAMPEX satellite observations of relativistic microbursts, primarily containing only relativistic electrons [e.g., *Blake et al.*, 1996]. It is expected that electron precipitation produced by VLF chorus will contain a wide range of electron energies [e.g., *Bortnik and Thorne*, 2007, Figure 3], which we examine in the next section.

5. Modeling of Chorus-Produced VLF Perturbations

[19] It is widely assumed that REP microbursts that have been observed on satellite particle detectors are due to wave-particle interactions with VLF chorus waves. The FAST perturbations were observed on the nightside, starting from ~1900 LT. In general chorus, which is widely believed to be the cause of relativistic microbursts, is normally associated with the morning sector. However, during highly disturbed geomagnetic conditions plasma sheet electrons will be injected into the nightside. This new population of ~1–10 keV electrons should "seed" chorus activity throughout the nightside and round into the morning sector as the electrons drift westward. Such a "cartoon picture" is consistent with the variation of equatorial chorus with geomagnetic activity, observed by the CRRES satellite [*Meredith et al.*, 2003]. Immediately before the onset of the 21 January 2005 storm, the broadband VLF receiver at Halley, Antarctica (76°S, 26°W, $L = 4.7$) was detecting VLF chorus (0.5–2 kHz) in the dayside/afternoon sector [*Clilverd et al.*, 2006]. While the Halley chorus disappeared at the storm onset time (1712 UT), this was probably as a result of increased ionospheric absorption of the chorus signal, rather than the chorus activity itself stopping. Further evidence for this comes from DEMETER-spacecraft VLF

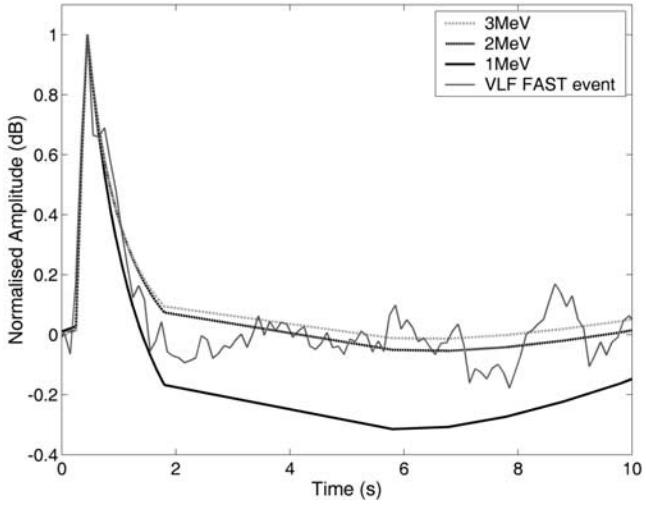

Figure 6. Comparison between the time-decay of the Sodanklya-observed FAST VLF perturbation from 5 April 2005, with those calculated due to monoenergetic 0.1 s REP bursts of varying energies (1, 2, 3 MeV).

observations made above Finland shortly after the start of the 21 January 2005 storm, in which chorus was observed [*Parrot*, 2006]. Thus it appears VLF chorus was occurring at least during the 21 January 2005 storm period and roughly in the location of our subionospheric receiver at Sodankylä.

[20] In order to test the subionospheric FAST observations against the expected signature for chorus-produced precipitation, we make use of calculated precipitation fluxes produced by a single chorus element using the modeling technique discussed in detail by *Bortnik et al.* [2006a, 2006b] and first applied to chorus by *Bortnik and Thorne* [2007], applied to the SIC and subionospheric propagation models in the same manner as the previous section. As described in the work of *Bortnik and Thorne* [2007], the modeling represents an ''average'' chorus element, with $f = 1–1.5$ kHz, rise time of 2 kHz/s and peak amplitude 10 pT. The chorus rays are launched from the geomagnetic equator. As these rays propagate, they resonate with counterstreaming energetic electrons. In the case of the dominant $m = 1$ resonance mode the interaction leads to precipitation of electrons at relatively low energies (e.g., ~100 keV). Note that the resonant mode will be dominant around the geomagnetic equator for a large range of wave normal angles. However, as these chorus waves propagate away from the geomagnetic equator, their wave-normal angles will become more oblique, such that higher-order resonances are also possible, including both counterstreaming and costreaming orientations. In our calculation we include resonance modes −5 to +5, which allow interactions with higher-energy electrons and hence the precipitation of MeV electrons.

[21] Observations from the Cluster spacecraft show that chorus has a source that moves rapidly along a geomagnetic field line but stays close to the geomagnetic equator [*Parrot et al.*, 2003]. Estimates of the scale of this movement are ~2000–3000 km, a very small fraction of the actual propagation length of each chorus element, which is several R_E. As most of the interactions between chorus elements and MeV electrons occurs away from the geomagnetic equator (>15°), the approximations used to describe our chorus source region will make no difference to the flux of very energetic electrons precipitated.

[22] Figure 7 shows the calculated precipitation fluxes at $L = 5$ impacting the northern hemisphere (Figure 7, top) and southern hemisphere (Figure 7, bottom) atmosphere at 100 km, caused by a single chorus element. The calculation is undertaken using a test particle simulation assuming AE-8 trapped electron flux levels and an isotropic distribution that is sharply cut off at the loss cone. In the northern hemisphere there are two energy groupings present in the precipitated flux, a low-energy group with intense fluxes from ~4 to 30 keV plus a high-energy high-flux group from ~150 keV to 4 MeV. The low-energy group corresponds to electrons which have undergone Landau (or longitudinal) resonance ($m = 0$), a costreaming interaction that will appear only in the northern hemisphere. The contrasting precipitation into the southern hemisphere is made up of a single high-energy grouping spanning ~50 keV to 3 MeV, with fluxes ~10 times larger than the peak flux in the Figure 7. These southern hemisphere calculations are also representative of the case for northern hemisphere precipitation due to a southward propagating chorus element.

[23] Once again, we make use of the SIC model to describe the impact of the chorus-generated precipitation, and subiosnopheric propagation and scattering modeling to consider the VLF signature expected in our narrowband observations. This is a useful test of whether the energies which resonate with VLF chorus could produce a VLF perturbation similar to that seen in January and April 2005. Figure 8 shows the time varying electron number density profiles determined from the SIC model due to the fluxes shown in Figure 7 (top) representing the chorus-driven precipitation at $L = 5$ into the northern hemisphere. Clearly, the significant population of nonrelativistic electrons leads to large, long-lived increases in the electron density profile at altitudes >70 km. Figure 9 shows the time-varying VLF perturbation due to the chorus burst shown in Figure 7. Clearly, the decay time of the chorus-driven perturbation is considerably longer than the 1.4 s observed, as emphasized by the contrast with the decay time for the same representative FAST perturbation (light line) shown in Figure 6. The large population of precipitating electrons with energies of hundreds of keV produce a long-lasting ionospheric modification at >70 km altitude, leading to the large negative perturbation for timescales >10 s. The time decay signature of the experimentally observed FAST VLF perturbations is much too short to be consistent with the precipitation caused by VLF chorus seen in Figure 9. No long-decay subionospheric VLF perturbations consistent with the calculations shown in Figure 9 were observed during the geomagnetic storms of 21 January or 4 April 2005.

[24] As shown in Figure 7, the modeled chorus-driven electron precipitation contains a wide range of electron energies, including simultaneous relativistic and nonrelativistic components. This is not the energy signature reported for REP microbursts, which have been observed on board satellites with no significant nonrelativistic population [e.g., *Blake et al.*, 1996]. Various modeling approaches can increase the calculated relativistic population in a modeled chorus-driven microburst; however, this also leads to an

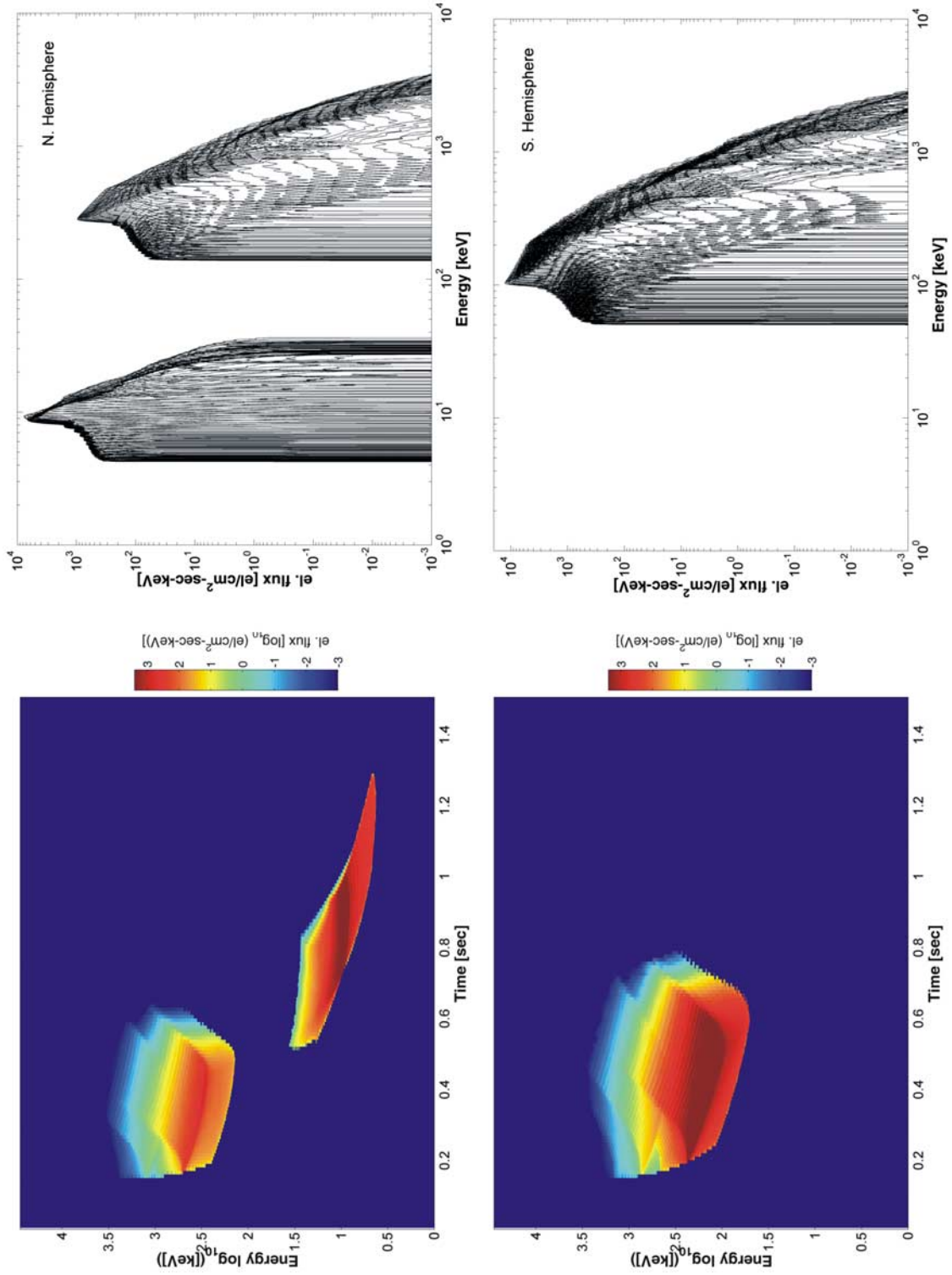

Figure 7. The calculated precipitation fluxes at $L = 5$ impacting the northern hemisphere atmosphere (top) at 100 km, caused by a single chorus element, and (bottom) the same information for the southern hemisphere.

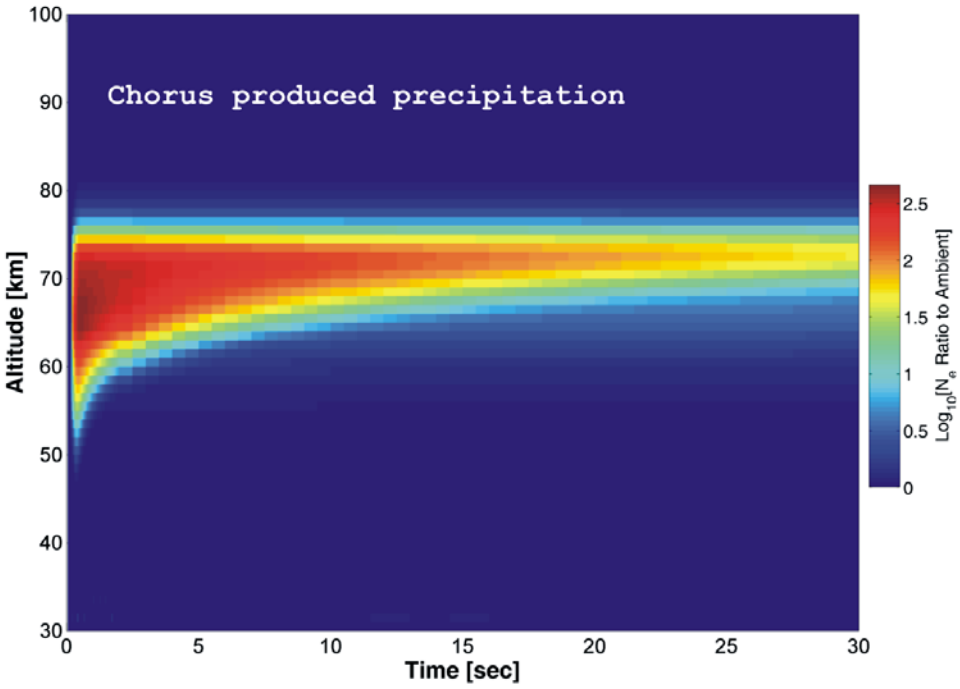

Figure 8. Time varying electron number density calculated by the SIC model, showing the decay of a chorus-produced ionospheric change due to the fluxes shown in Figure 7, top.

increase in the nonrelativistic population. There is no realistic combination of parameters describing VLF chorus that will remove the ~100 keV precipitated electron component while retaining any relativistic fluxes. While we acknowledge that there may be some room to adjust the ratio of <100 keV relative to the >1 MeV fluxes, the <100 keV fluxes will always be dominant in the precipitation spectrum and ionospheric decay time, producing a microburst which is more consistent with the nonrelativistic microburst observations [e.g., *Reinard et al.*, 1997], known to be linked to VLF chorus [*Rosenberg et al.*, 1990], than the REP microbursts which have to date only been associated with chorus. Both the satellite observations of typical REP microbursts containing no significant nonrelativistic component and the VLF FAST perturbation decay times agree but are inconsistent with VLF chorus as the primary precipitation driver (as we currently model it).

6. Discussion and Summary

[25] On 21 January 2005 a $Kp = 8$, $Dst = -100$ nT geomagnetic storm occurred, leading to a relativistic electron dropout at geosynchronous orbit starting at ~1710 UT. Over the following ~4 hours several hundred short-lived VLF perturbations were observed by the AARDDVARK receiver in Sodankylä, Finland. The vast majority of these perturbations were not simultaneous with perturbations on other nearby paths, even though they occurred during the same periods, consistent with a precipitation "rainstorm" producing ionospheric changes of small spatial sizes around the Sodankylä receiver. During another time period containing short-lived VLF perturbations but no SPE or "SLOW" REP perturbations, the decay time was ~1.2 s, which we take as the "true" decay time of the FAST perturbations. This decay time is consistent with short-lived bursts of highly relativistic electrons, precipitating into the atmosphere. In neither of the study periods considered here were the FAST perturbations accompanied by those expected from nonrelativistic microbursts, which would take >60 s to recover.

[26] Further studies into the nature of the disturbed ionosphere, including more detailed investigation of the microburst energy spectrum will require new VLF propagation codes which can accurately model the absolute amplitude and phase response of an intense ionospheric disturbance located close to the receiver. Such codes are under development [e.g., *McCormick et al.*, 2005].

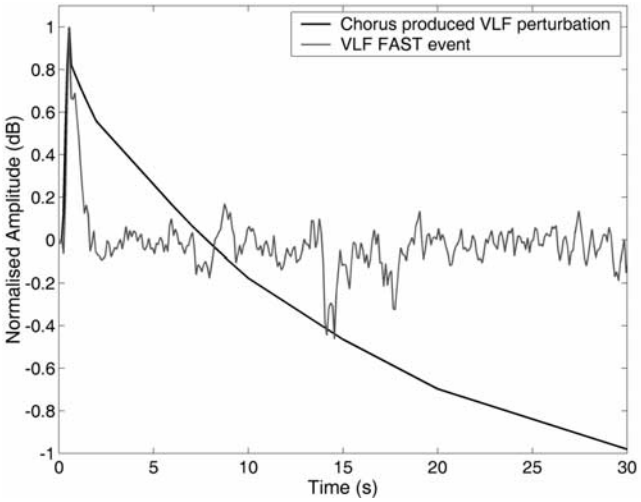

Figure 9. Time varying VLF perturbation produced by a chorus-driven precipitation spectra, to be contrasted with the same observed FAST VLF perturbation from Figure 6.

[27] Contrasts between the predicted VLF perturbations expected for chorus-driven precipitation and those due to more highly energetic beams indicate that the recovery time is most consistent with precipitation containing only highly relativistic populations, principally from energies greater than about 2 MeV. This agrees with satellite observations of the microburst energy spectrum. The chorus-driven VLF perturbations calculated were very unlike the experimentally observed FAST VLF perturbations and also unlike the reported typical energy spectra of satellite observed relativistic microbursts (e.g., SAMPEX). While it is widely assumed that REP microbursts are due to wave-particle interactions with VLF chorus waves, our results suggest that this may not be the case. We caution that the events we are considering occur during intense geomagnetic disturbances posing additional challenges to theorists and also note that since the modeling of relativistic electron microbursts with our technique is in its infancy, there is still much work to be done in fully understanding this phenomenon. The results inferred from satellite and subionospheric observations, namely the absence of a large, dominant component of <100 keV precipitating electrons, fundamentally disagrees with a mechanism of chorus-driven precipitation. Nonetheless, further work on the modeling of chorus-driven precipitation is required.

[28] One should also consider other possibilities for the differences between the chorus-driven precipitation modeling and the FAST VLF perturbations reported here. One possibility is that the short-lived and relativistic precipitation bursts occurring around our Sodankylä receiver are somehow different from "typical" REP mirobursts, allowing the postulation to remain that typical REP microbursts are caused by VLF chorus. However, this seems unlikely, especially given that the satellite REP microburst spectrum is highly consistent with that required to produce our VLF observations, while the calculated chorus-driven precipitation (Figure 7) has a very different energy spectrum than reported by satellites for REP microbursts. At this point the most likely conclusion is that satellite-observed REP microbursts are not produced by wave-particle interactions with VLF chorus waves, as is widely assumed.

[29] At this stage we cannot conclude that the FAST subionospheric VLF perturbations are caused by the same relativistic electron microbursts as previously observed from satellite. The SAMPEX satellite did not observe REP microbursts during the 21 January 2005 storm (R. M. Millan, personal communication, 2006), but also was not located near the longitude sector of our Finnish receiver. Nonetheless, the most likely explanation for the FAST subionospheric VLF perturbations is short-lived bursts of electron precipitation, principally with energies >2 MeV. We plan a wider study to investigate the magnetic local time variation of FAST VLF perturbations and hence construct a database to allow comparison with in situ satellite measurements of precipitation. The energetic nature of the precipitation which produces the FAST perturbations suggests that they should be observable in both day and night conditions.

[30] **Acknowledgments.** C. J. R. would like to thank Anne Rodger of Mosgiel, New Zealand, for her support, Michelle F. Thomsen of Los Alamos National Laboratory, and Paul O'Brien of The Aerospace Corporation for helpful discussions.

[31] Zuyin Pu thanks Bernard Blake and another reviewer for their assistance in evaluating this paper.

References

Anderson, K. A., and D. W. Milton (1964), Balloon observations of X-rays in the auroral zone: 3. High time resolution studies, *J. Geophys. Res.*, *69*, 4457.

Barr, R., D. L. Jones, and C. J. Rodger (2000), ELF and VLF radio waves, *J. Atmos. Sol. Terr. Phys.*, *62*(17–18), 1689–1718.

Blake, J. B., M. D. Looper, D. N. Baker, R. Nakamura, B. Klecker, and D. Hovestadt (1996), New high temporal and spatial resolution measurements by SAMPEX of the precipitation of relativistic electrons, *Adv. Space Res.*, *18*(8), 171–186.

Bortnik, J., and R. M. Thorne (2007), The dual role of ELF/VLF chorus waves in the acceleration and precipitation of radiation belt electrons, *J. Atmos. Sol. Terr. Phys.*, *69*(3), 378–386.

Bortnik, J., U. S. Inan, and T. F. Bell (2006a), Temporal signatures of radiation belt electron precipitation induced by lightning-generated MR whistler waves: 1. Methodology, *J. Geophys. Res.*, *111*, A02204, doi:10.1029/2005JA011182.

Bortnik, J., U. S. Inan, and T. F. Bell (2006b), Temporal signatures of radiation belt electron precipitation induced by lightning-generated MR whistler waves: 2. Global signatures, *J. Geophys. Res.*, 111, A02205, doi:10.1029/2005JA011398.

Clilverd, M. A., R. F. Yeo, D. Nunn, and A. J. Smith (1999), Latitudinally dependent Trimpi effects: Modeling and observations, *J. Geophys. Res.*, *104*(A9), 19,881–19,887.

Clilverd, M. A., C. J. Rodger, and T. Ulich (2006), The importance of atmospheric precipitation in storm-time relativistic electron flux drop outs, *Geophys. Res. Lett.*, *33*, L01102, doi:10.1029/2005GL024661.

Cummer, S. A. (2000), Modeling electromagnetic propagation in the earth-ionosphere waveguide, *IEEE Trans. Antennas Propag.*, *48*(9), 1420–1429.

Datta, S., R. M. Skoug, M. P. McCarthy, and G. K. Parks (1996), Analysis and modeling of microburst precipitation, *Geophys. Res. Lett.*, *23*, 1729–1732.

Dowden, R., C. Rodger, J. Brundell, and M. Clilverd (2001), Decay of whistler-induced electron precipitation and cloud-ionosphere discharge Trimpis: Observations and analysis, *Radio Sci.*, *36*(1), 151–169.

Imhof, W. L., H. D. Voss, J. Mobilia, M. Walt, U. S. Inan, and D. L. Carpenter (1989), Characteristics of short-duration electron precipitation bursts and their relationship with VLF wave activity, *J. Geophys. Res.*, *94*, 10,079.

Imhof, W. L., H. D. Voss, J. Mobilia, D. W. Datlowe, E. E. Gaines, J. P. McGlennon, and U. S. Inan (1992), Relativistic electron microbursts, *J. Geophys. Res.*, *97*, 13,829–13,837.

Lee, J.-J., et al. (2005), Energy spectra of (170–360 keV electron microbursts measured by the Korean STSAT-1, *Geophys. Res. Lett.*, *32*, L13106, doi:10.1029/2005GL022996.

Lorentzen, K. R., M. D. Looper, and J. B. Blake (2001a), Relativistic electron microbursts during the GEM storms, *Geophys. Res. Lett.*, *28*(13), 2573.

Lorentzen, K. R., J. B. Blake, U. S. Inan, and J. Bortnik (2001b), Observations of elativistic electron microbursts in association with VLF chorus, *J. Geophys. Res.*, *106*(A4), 6017–6027.

McCormick, R. J., D. Nunn, C. J. Rodger, and N. R. Thomson (2005), Full wave VLF subionospheric modelling with spherical geometry, paper presented at 28th General Assembly, Int. Union of Radio Sci., Ghent, Belgium.

Meredith, N. P., R. B. Horne, R. M. Thorne, and R. R. Anderson (2003), Favored regions for chorus-driven electron acceleration to relativistic energies in the Earth's outer radiation belt, *Geophys. Res. Lett.*, *30*(16), 1871, doi:10.1029/2003GL017698.

Millan, R. M., R. P. Lin, D. M. Smith, K. R. Lorentzen, and M. P. McCarthy (2002), X-ray observations of MeV electron precipitation with a balloon-borne germanium spectrometer, *Geophys. Res. Lett.*, *29*(24), 2194, doi:10.1029/2002GL015922.

Morfitt, D. G., and C. H. Shellman (1976), MODESRCH, an improved computer program for obtaining ELF/VLF/LF propagation data, *Naval Ocean Systems Center Tech. Rep. NOSC/TR 141, NTIS Access. ADA047508*, Natl. Tech. Inf. Serv., Springfield, Va.

Nakamura, R., M. Isowa, Y. Kamide, D. N. Baker, J. B. Blake, and M. Looper (2000), SAMPEX observations of precipitation bursts in the outer radiation belt, *J. Geophys. Res.*, *105*(A7), 15,875.

Nunn, D. (1997), On the numerical modelling of the VLF Trimpi effect, *J. Atmos. Sol. Terr. Phys.*, *59*, 537–560.

Nunn, D., and C. J. Rodger (1999), Modeling the relaxation of red sprite plasma, *Geophys. Res. Lett.*, *26*(21), 3293–3296.

Nunn, D., and H. J. Strangeways (2000), Trimpi perturbations from large ionisation enhancement patches (LIEs), *J. Atmos. Sol. Terr. Phys.*, *62*(3), 189–206.

O'Brien, T. P., M. D. Looper, and J. B. Blake (2004), Quantification of relativistic electron microburst losses during the GEM storms, *Geophys. Res. Lett.*, *31*, L04802, doi:10.1029/2003GL018621.

Parrot, M. (2006), Survey of ELF/VLF waves observed by DEMETER above Finland, *Sodankylä Geophys. Obs. Rep. 56*, edited by J. Manninen, T. Ulich, and A.-L. Piippo, p. 33, Sodankylä Geophys. Obs., Sodankylä, Finland.

Parrot, M., O. Santolk, N. Cornilleau-Wehrlin, M. Maksimovic, and C. C. Harvey (2003), Source location of chorus emissions observed by Cluster, *Ann. Geophys.*, *21*, 473–480.

Reeves, G. D., K. L. McAdams, R. H. W. Friedel, and T. P. O'Brien (2003), Acceleration and loss of relativistic electrons during geomagnetic storms, *Geophys. Res. Lett.*, *30*(10), 1529, doi:10.1029/2002GL016513.

Reinard, A. A., R. M. Skoug, S. Datta, and G. K. Parks (1997), Energy spectral characteristics of auroral electron microburst precipitation, *Geophys. Res. Lett.*, *24*, 611–614.

Rishbeth, H., and O. K. Garriott (1969), *Introduction to Ionospheric Physics*, Academic, San Diego, Calif.

Rodger, C. J., and R. J. McCormick (2006), Remote sensing of the upper atmosphere by VLF, in *Sprites, Elves and Intense Lightning Discharges*, *Nato Sci. Ser. II*, vol. 225, edited by M. Füllekrug, pp. 167-190, Springer, New York.

Rodger, C. J., D. Nunn, and M. A. Clilverd (2004), Investigating radiation belt losses though numerical modelling of precipitating fluxes, *Ann. Geophys.*, *22*(10), 3657–3667.

Rosenberg, T. J., R. Wei, D. L. Detrick, and U. S. Inan (1990), Observations and modeling of wave-induced microburst electron precipitation, *J. Geophys. Res.*, *95*(A5), 6467–6475.

Seppälä, A., P. T. Verronen, V. F. Sofieva, J. Tamminen, E. Kyrölä, C. J. Rodger, and M. A. Clilverd (2006), Destruction of the tertiary ozone maximum during a solar proton event, *Geophys. Res. Lett.*, *33*, L07804, doi:10.1029/2005GL025571.

Thorne, R. M., T. P. O'Brien, Y. Y. Shprits, D. Summers, and R. B. Horne (2005), Timescale for MeV electron microburst loss during geomagnetic storms, *J. Geophys. Res.*, *110*, A09S32, doi:10.1029/2004JA010882.

Turunen, E., H. Matveinen, J. Tolvanen, and H. Ranta (1996), D-region ion chemistry model, in *STEP Handbook of Ionospheric Models*, edited by R. W. Schunk, pp. 1–25, SCOSTEP Secretariat, Boulder, Colo.

Verronen, P. T., E. Turunen, T. Ulich, and E. Kyrölä (2002), Modelling the effects of the October 1989 solar proton event on mesospheric odd nitrogen using a detailed ion and neutral chemistry model, *Ann. Geophys.*, *20*, 1967–1976.

Verronen, P. T., A. Seppälä, M. A. Clilverd, C. J. Rodger, E. Kyrölä, C. Enell, T. Ulich, and E. Turunen (2005), Diurnal variation of ozone depletion during the October–November 2003 solar proton events, *J. Geophys. Res.*, *110*, A09S32, doi:10.1029/2004JA010932.

Wait, J. R. (1996), *Electromagnetic Waves in Stratified Media*, IEEE Press, New York.

Wait, J. R., and K. P. Spies (1964), Characteristics of the Earth-ionosphere waveguide for VLF radio waves, *NBS Tech. Not. 300*, Natl. Inst. of Stand. and Technol., Gaithersburg, Md.

Watt, A. D. (1967), *VLF Radio Engineering*, Elsevier, New York.

J. Bortnik, Department of Atmospheric and Oceanic Sciences, University of California, Los Angeles, Los Angles, CA 90095, USA.

M. A. Clilverd, Physical Sciences Division, British Antarctic Survey, High Cross, Madingley Road, Cambridge CB3 0ET, UK.

D. Nunn, School of Electronics and Computer Science, Southampton University, Highfield, Southampton S917 1BJ, UK.

C. J. Rodger, Department of Physics, University of Otago, P.O. Box 56, Dunedin, New Zealand. (crodger@physics.otago.ac.nz)

E. Turunen, Sodankylä Geophysical Observatory, University of Oulu, FIN-99600 Sodankylä, Finland.

P. T. Verronen, Earth Observation, Finnish Meteorological Institute, P.O. Box 503, FIN-00101 Helsinki, Finland.